ORIGINAL ARTICLE

Preparation and evaluation of binary and ternary inclusion complexes of fenofibrate/hydroxypropyl-β-cyclodextrin

Xizhao Ding[1] · Mengke Zheng[2] · Jiamin Lu[2] · Xingyi Zhu[1,2]

Abstract

This study aimed to investigate the effect of hydroxypropyl methylcellulose on the complexation of fenofibrate and hydroxypropyl-β-cyclodextrin (HP-β-CD). Initially, phase solubility studies with an excess amount of drug in the HP-β-CD solutions with and without hydroxypropyl methylcellulose (HPMC) were investigated. Both of the binary and ternary complexes were prepared by ball-milling. The complexes were characterized by Fourier transform infrared spectroscopy (FI-IR), X-ray powder diffraction (XPRD), differential scanning calorimetry (DSC) and nuclear magnetic resonance spectroscopy (^{1}H-NMR). The A_L type phase-solubility diagram revealed that the complexes of fenofibrate and HP-β-CD were formed with molecular ratio of 1:1. The results of FT-IR, XPRD, DSC and ^{1}H NMR analysis show the formulation of inclusion complexes. In conclusion, the interaction occurrs between fenofibrate and HP-β-CD in the complexes, and the existence of HPMC effectively improves the complexation efficiency and stability constant. The in vitro dissolution test suggests ternary complex is superior to binary complex in terms of the release of fenofibrate.

Keywords Fenofibrate · Hydroxypropyl-β-cyclodextrin · Hydroxypropyl methylcellulose · Phase-solubility study · Complexes

Introduction

Fenofibrate (FNB), also known as proulrine is a pro-drug of fenofibrate acid, which has an irreplaceable status in clinical applications as a potentional lipid-lowering drug [1]. It is widely used in the treatment of hypertriglyceridemia and mixed hyperlipidemia [2, 3]. Fenofibrate is a typical drug of Biopharmaceutics Classification System (BCS) class II compounds with high permeability and low solubility. A variety of measurements have been taken to improve solubility and bioavailability of these drugs, such as reducing the particle size or the crystallinity of the drugs, increasing its surface area, preparing for liposomes and so on [4–6].

Cyclodextrins are cyclic oligosaccharides with hydrophilic surface and hydrophobic central cavity, which are favored the formation of inclusion complexes with low polarity drugs, therefore, they have been widely used as the excipients of the inclusion compounds to improve drug solubility [7, 8]. Hydroxypropyl-β-cyclodextrin (HP-β-CD) is one of the cyclodextrin derivatives which have several advantages than other cyclodextrins such as well water-solubility, well tolerated in animals, excellent absorption, high bioavailability, strong solubilization, excellent stability, less toxicity and irritation of tissues. So it has received frequent usage as pharmaceutical solubilizers, excipients and so on [9, 10]. Additionally, Food and Drug Administration (FDA) has approved the use of HP-β-CD as solubilizer for itraconazole injection and levonorgestrel long-acting subcutaneous implants. The documentation of pharmacological and toxicological tests for the existing animals show that the safety of the HP-β-CD is guaranteed basically [11, 12].

In recent years, because of the low complexation efficacy of the cyclodextrins, many studies has been carried out to overcome this disadvantage, for instance, the addition of small amounts of hydrophilic polymers, hydroxyl acids or amino acids as complexation media to produce

✉ Xingyi Zhu
zxy@zjut.edu.cn

1 College of Pharmaceutical Sciences, Zhejiang University of Technology, No.18 Chaowang Road, Hangzhou 310014, China

2 Collaborative Innovation Center of Yangtze River Delta Region Green Pharmaceuticals, Zhejiang University of Technology, No.18 Chaowang Road, Hangzhou 310014, China

ternary complexes [13–15]. Some approaches have already been reported to increase the solubility and dissolution rate of FNB, such as solid dispersion, nanosuspension and CD complexation [16]. Therefore, the aim of this study was to enhance its solubility and dissolution rate by developing ternary complexes of FNB and HP-β-CD with the existence of HPMC.

Materials and methods

Materials

Fenofibrate (FNB, purity ≥ 98%) was supplied by Shanghai Yi Jing industry Co., Ltd. (Shanghai, China); hydroxypropyl-β-cyclodextrin was purchased from Qianhui Fine Chemical Co., Ltd. (Zibo, China); hydroxypropyl methyl cellulose (HPMC) was supplied by Shanhe Medicinal Materials Co., Ltd. (Anhui, China); sodium dodecyl sulfate (SDS) and acetonitrile were obtained from Sinopharm Group Chemical Reagent Co., Ltd. (Beijing, China).

Preparation of complexes

Phase-solubility studies

The effect of HP-β-CD on the solubility of FNB in water was studied using the phase solubility method. A series concentration (1, 5, 10, 15, and 20% w/v) of HP-β-CD solutions with excess FNB were prepared. The experiments for ternary systems were performed with the addition of HPMC analogously to binary systems. Then the solution was shocked in constant temperature water bath shaker for 48 h at different temperature respectively (25, 37, and 40 ± 0.5 °C), and the shocking speed was 150 rpm. The solution was filtered through 0.45 µm microporous membrane after equilibrium. The filtered liquor was detected by HPLC to calculate the drug concentration, and each sample was measured three times in parallel.

The phase-solubility curves were plotted with the concentration of the HP-β-CD solution as the abscissa and the concentration of FNB as the ordinate, and then the slope was calculated.

Phase-solubility analysis is a traditional approach to investigate the effect of complexing agents on the solubilized compound. It determines not only the value of the stability constant but also giving insight into the stoichiometry of the equilibrium. Based on the shape of the generated phase-solubility relationships, several types of behaviors could be identified. A_L profile indicates a linear increase in solubility due to the function of solubilizer. It also suggests that the drug forms tolerable inclusion with HP-β-CD. On the contrary, type B phase-solubility profile indicates the formation of complexes with limited water solubility. If the drug forms the A_L-type relationships, they are first order with respect to the HP-β-CD and may be first of higher order with respect to the drug. If the slope of the phase diagram is less than 1, a one-to-one complex is often assumed in the absence of other information; if the slope of the phase diagram is greater than 1, higher order complexes are assumed to be involved in the solubilization [17–19].

Complexes of FNB/HP-β-CD and FNB/HP-β-CD/HPMC by ball-milling

Both of the inclusion complexes were prepared by ball milling. The FNB and HP-β-CD (molar ratio 1:1) were put into stainless steel jar which was added a third tank volume of steel balls with the diameter of 12 mm. The complexes were milled using planetary ball mill (Retsch, Verder Shanghai Instruments and Equipment Co., Ltd.) for 90 min with speed of 200 rpm, the co-milled product screened with 100 mesh sieve and the binary inclusion complex was obtained. The ternary system was procured in the same way with adding a spot of HPMC. Othewise, the physical mixture in the same ratio was obtained to be contrast.

Establishment of FNB analysis method

The concentration of FNB was determined using the high performance liquid chromatography (Agilent-1200 Shimadzu, Racing Technology Co., Ltd Hangzhou, China), chromatographic analysis was investigated on C18 analytical column (Eclipse, 4.6 × 150 mm, 5 µm), with acetonitrile/water (85:15, v/v) as the mobile phase and UV detection at 286 nm. The measurement temperature was 25 °C, the injection volume was 5 µl and the flow rate was 1 ml/min.

Differential scanning calorimetry (DSC)

A baseline was used as a background prior to DSC analysis. The DSC curves of the samples were measured with differential scanning calorimeter (Mettler Q100 apparatus TA Corporation, USA). Samples were heated in a sealed aluminium pan from 20 to 200 °C at the rate of 10 °C/min under a nitrogen flow of 40 ml/min. An empty sealed pan was used as the reference.

Fourier transform infrared spectroscopy (FI-IR)

The FI-IR spectra was acquired by Avatar 330 Fourier transform infrared spectroscopy (Thermo Niclolet Corporation, USA) from 4000 to 400 cm^{-1}, with the collection at resolution of 4 cm^{-1} at room temperature. The samples were prepared by mixing 2% (w/w) of the powders in potassium bromide (KBr).

X-ray powder diffraction experiment (XPRD)

XPRD patterns of all samples (5 mg each) were recorded to determine the crystallinity changes and/or polymorphic transformations if any, by using an X-ray diffraction spectrometer (PANalytical B.V., Holland). The diffractograms were recorded at a scanning speed of 10 °C/min with the source of Cu and chart speed of 0.05° per 2 theta range from 1° to 80°, stay for 15 s.

Nuclear magnetic resonance spectroscopy (^{1}H-NMR)

The one-dimensional ^{1}H NMR of the samples was conducted with 600 MHz Mercury pLUS-400 NMR spectrophotometer (Varian Corporation, USA) at 25 °C. And 0.5 ml of DMSO-d6 was used as the dissolvant.

In vitro dissolution study

In vitro dissolution rate of the samples was tested according to the second method (pulp method) for the dissolution determination of the Chinese Pharmacopoeia (2015). In vitro dissolution tests were obtained by HTY-EU802 rotating paddle apparatus (Tailin Bioengineering Equipments Co., Ltd., Hangzhou) at 37 ± 0.5 °C with 900 ml of 0.5% (w/v) SDS as the dissolution medium, and the stirring speed was 75 rpm. The samples (10 ml) were withdrawn at predetermined time intervals (5, 10, 20, 30, 45 and 60 min), meanwhile adding the equal volume of fresh dissolution medium. After the samples were filtered with 0.45 μm microporous membrane, 5 ml of filtrate was collected and detected by HPLC to calculate the content.

Results and discussion

Experimental analysis of phase solubility

Solubility of FNB in HP-β-CD solution at different temperatures with and without HPMC was shown in Figs. 1 and 2. The solubility of FNB in water increased linearly with the increasing of HP-β-CD concentration at the temperature of 25 °C, 37 °C and 40 ± 0.5 °C, as described earlier, this profile could be classified as A_L-type diagram. The diagram is still A_L-type diagram with the presence of HPMC, all of the slope is less than 1. Therefore, the inclusion compound at a molar ratio of 1:1 was formed between FNB and HP-β-CD both in binary and ternary system.

According to the phase solubility curves, the stability constants of complexes (Ks) and complexation efficiency (CE) at different temperatures were calculated based on the obtained experimental data by Eqs. (1 and 2) [20],

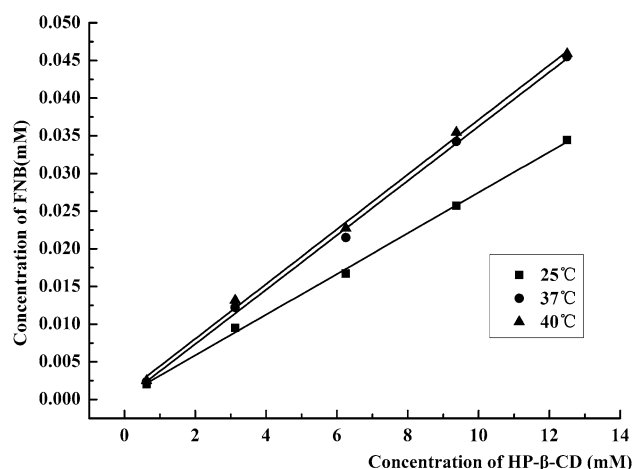$$Ks = \frac{slope}{D_0(1 - slope)} \qquad (1)$$

Fig. 1 Phase-solubility diagram of FNB in the presence of HP-β-CD in water at 25, 37, and 40 °C

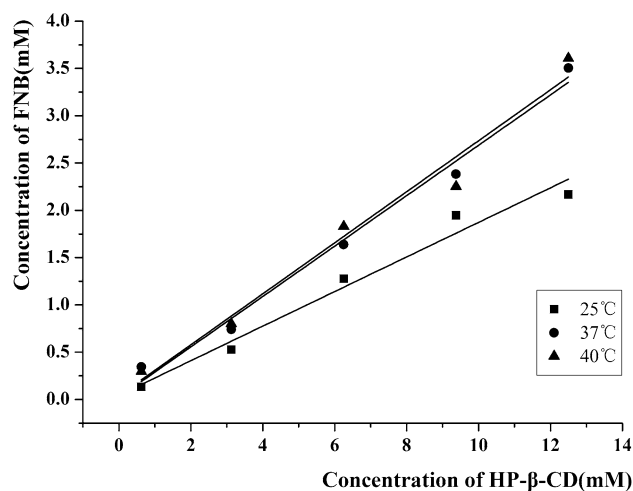**Fig. 2** Phase-solubility diagram of FNB in HP-β-CD solution with HPMC at 25, 37, and 40 °C

$$CE = \frac{slope}{1 - slope} \qquad (2)$$

where D_0 is the intrinsic solubility of FNB in purified water, slope is the initial upward linear portion of the phase solubility curve. The parameter values of Eqs. (1 and 2) were shown in Table 1.

Ks values for binary systems at different temperature were 4.7823×10^3, 5.4904×10^3, and 5.4582×10^3 M^{-1}, respectively. On the contrary, the values were 397.7990×10^3, 551.8391×10^3, and 557.6190×10^3 M^{-1} in ternary system. The comparison shows that the presence of HPMC has enhanced the stability of the complex obviously. Similarly, the complexation efficiency (CE) of ternary system is much

Table 1 The values of the parameter of equation and the stability constants of the FNB/HP-β-CD inclusion complex and FNB/HP-β-CD/HPMC inclusion complex

T (K)	Slope	D_0 (µg/ml)	$K_{SB} \times 10^3$ (M^{-1})	$K_{ST} \times 10^3$ (M^{-1})	CE_B	CE_T
298.15	0.0027	0.2023	4.7823	397.7990	0.0027	0.2235
310.15	0.0036	0.2369	5.4904	551.8389	0.0036	0.2737
313.15	0.0036	0.2383	5.4582	557.6190	0.0036	0.3691

Slope the slope of the phase solubility curves; D_o the saturated solubility of enofibrate in different temperature; K_{SB} the stability constants of FNB/HP-β-CD complex; K_{ST} the stability constants of FNB/HP-β-CD/HPMC complex; CE_B the complexation efficiency of FNB/HP-β-CD complex; CE_T the complexation efficiency of FNB/HP-β-CD/HPMC complex

Table 2 Thermodynamic parameters of inclusion complex in binary and ternary system

Thermodynamic parameters	ΔG (kJ/mol)	ΔH (kJ/mol)	ΔS [J/(mol K^{-1})]
Binary system	− 21.8697	− 7.4161	48.4776
Ternary system	− 33.5003	− 18.4654	50.4273

Binary system the inclusion complex of FNB and HP-β-CD; *ternary system* the inclusion complex of FNB, HP-β-CD and HPMC; *ΔG* Gibbs free energy; *ΔH and ΔS* enthalpy and entropy of complex formation

higher than that of binary complex, which indicates relatively strong interactions have formed between FNB and the HP-β-CD with adding HPMC. The increased complex stability of cyclodextrin and the drug could be attributed to the interactions established in the molecules, such as Van der Waals dispersion forces, hydrophobicbonds, hydrogen bonds and the release of high-energy water molecules presenting in the HP-β-CD cavity [21].

In addition, the thermodynamic parameters of inclusion complexes formation of the studied compounds were calculated from the Eqs. (3–5) according to the literature [22, 23],

$$\ln K_s = -\frac{\Delta H}{R \times T} + \frac{\Delta S}{R} \qquad (3)$$

$$\Delta G = -R \times T \times \ln K_S \qquad (4)$$

$$\Delta G = \Delta H - T \times \Delta S \qquad (5)$$

where Ks is the stability constant of the complex at the corresponding temperature, and ΔG is Gibbs free energy, ΔH and ΔS are enthalpy and entropy of complex formation, respectively, and R is gas constant.

The thermodynamic parameters of binary and ternary inclusion complexes were represented in Table 2. From the data in the table, the ΔG was negative either with or without HPMC which indicates that the inclusion process of FNB and HP-β-CD is a spontaneous process. Besides, the negative ΔH value and positive ΔS of the complexes were calculated, so the complex process was accompanied by heat release. The ΔG and ΔH of ternary complex were lower than
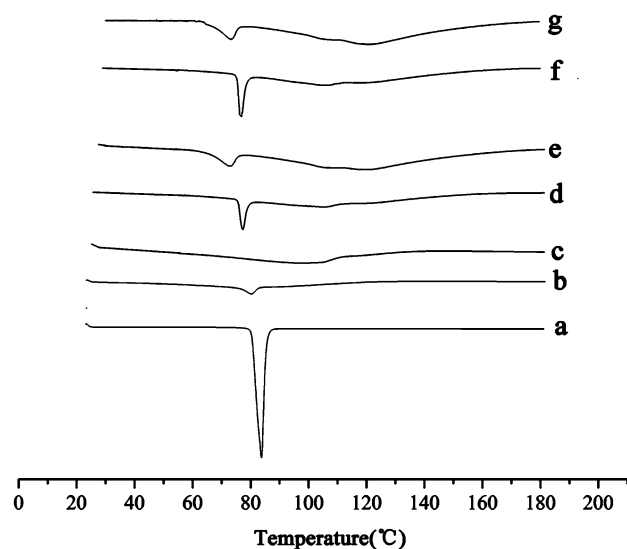
Fig. 3 Differential scanning calorimetry of FNB (**a**), HP-β-CD (**b**), HPMC (**c**), binary physical mixture (**d**), binary complex (**e**), ternary physical mixture (**f**) and ternary complex (**g**)

that of binary complex, which suggests the complexation is more likely to occur in the ternary system. Since the reaction process is enthalpy-driven when ΔS and ΔH are both positive or ΔH was highly negative [24, 25], the encapsulation process of FNB and HP-β-CD is considered to be a spontaneous and entropy-driven reaction process. Briefly, the complex of FNB and HP-β-CD can occur spontaneously and accompany by heat release.

DSC analysis

DSC curves are useful to explore inclusion complexes because an absence of an endothermic peak corresponds to the melting of the guest molecule, which indicates the formation of the complex. It can be seen that FNB has a significant absorption peak at 82 °C (Fig. 3a), according to Sailaja et al. has reported previously, it is resulted by the melting of FNB [26]. The powder of HP-β-CD (Fig. 3b) has a broad endothermic effect between 53 and 100 °C, which attributed to the loss of water molecules in the cavity of the

HP-β-CD as mentioned in the previous literature [27]. The DSC thermogram of HP-β-CD without the melting endotherm showed its amorphous form. The physical mixture of FNB and HP-β-CD indicated a distinct melting peak of FNB at 82 °C either with or without HPMC (Fig. 3e, g). On the contrary, patterns of the inclusion complexes show a small endothermic peak at 74.4 °C (Fig. 3d) of the binary system and 74.8 °C (Fig. 3f) of the ternary system. The position of the endothermic peak is different from the melting peak of FNB and the dehydration of HP-β-CD. This indicates that, the structure of the compounds has been changed and the inclusion complexes have been formed, and the endothermic peak is changed due to the molecular interaction.

FI-IR analysis

In order to determine whether there is an intermolecular interaction between FNB and HP-β-CD, the FI-IR spectrum was used for verification. The FI-IR spectrums were shown in Fig. 4. Character absorption peaks of FNB were founded at 1729.53 and 1651.08 cm^{-1} (Fig. 4a), one of them from the C=O vibration absorption and the other from methyl ester carbonyl group. The pattern of HP-β-CD shows vibration absorption peaks at 2927.42 and 1046.86 cm^{-1} attributed to the stretch of C–H and C–O–C respectively, and another peak at 1635.31 cm^{-1} (O–H, H bonded) is deformation vibration of the O–H bonds in the C–O–H groups and the water molecules. The peaks of FNB at 1729.53, 1651.08 cm^{-1} were moved to 1729.01, 1651.32 cm^{-1} (Fig. 4e) in binary inclusion complex and 1732.98, 1653.83 cm^{-1} (Fig. 4f) in ternary system. The peaks of HP-β-CD at 2927.42, 1046.86 cm^{-1}
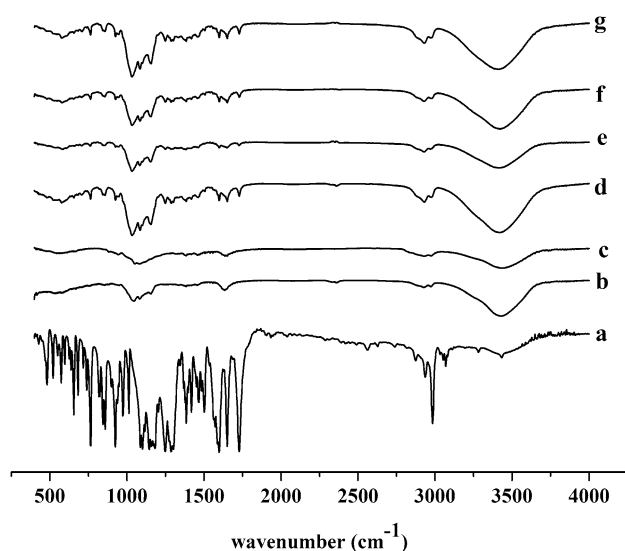
were shifted to 2930.52, 1033.52 cm^{-1} (Fig. 4e) in binary system and 2926.65, 1033.74 cm^{-1} (Fig. 4f) in ternary system, respectively.

Besides, the intensity of FNB characteristic absorption peaks in the inclusion complexes was significantly decreased and the peak shape was broadened. It suggested an interaction had occurred between FNB, HP-β-CD and HPMC, which resulted in decrease of the peak displacement and intensity. Moreover, the peak of HP-β-CD at 1635.31 cm^{-1} which belongs to the crystallization water was absent in the spectra of the complexes. All of the modification of the peaks might demonstrate that FNB entered into the cavity of HP-β-CD and replaced the water molecule inside the cavity, the inclusion complexes were formed.

XRD analysis

XRD is an effective method for the crystal state detection of the inclusion powder. If the drug and HP-β-CD inclusion complex has been formed, the diffraction peaks of the complex and the diffraction peak of each component in the inclusion compound are significantly different. Crystal powder diffraction pattern of FNB showed characteristic diffraction peaks at the diffraction angle of 14.64°, 16.32°, 22.40°, 26.44°, 29.12° and 30.64° (Fig. 5a), it demonstrates that FNB is presented in the form of crystals before co-milling. A typical halo-pattern noted in the spectra of HP-β-CD shows its amorphous character. The XRD patterns of the binary and ternary physical mixture exhibited the characteristic peaks of FNB (Fig. 5d, f). It is important to note that these peaks resulted from the combination of both pure components analyzed; hence there is no complex formation in physical mixture. On the contrary, the crystal diffraction peaks of FNB have changed evidently in the spectrum of inclusion complexes prepared by ball-milling (Fig. 5e, g), the relative degree of crystallinity decreased significantly compared with the pure drug. All of the variations could be attributed to the crystallographic modifications by the formulation of complexes and the crystalline nature changes into an amorphous form.

^{1}H NMR analysis

The inclusion mechanism of FNB and HP-β-CD was further explored by NMR spectroscopy. Inclusion of FNB molecule going into the hydrophobic cavity of the HP-β-CD will result in the change of chemical shift with HP-β-CD molecules in the ^{1}H NMR spectra. Chemical shifts of FNB and HP-β-CD protons with or without HPMC were shown in Tables 3 and 4. It could be seen that the H-3 and H-5 protons, located inside the cavity of HP-β-CD, were evidently shifted upfield in both binary and ternary system compared with the shifts of H-2 and H-4 which were located outside

Fig. 4 FI-TR spectrum of FNB (**a**), HP-β-CD (**b**), HPMC (**c**), binary physical mixture (**d**), binary complex (**e**), ternary complex (**f**) and ternary physical mixture (**g**)

Fig. 5 X-ray powder diffraction patterns of FNB (**a**), HP-β-CD (**b**), HPMC (**c**), binary complex (**d**), binary physical mixture (**e**), ternary complex (**f**) and ternary physical mixture (**g**)
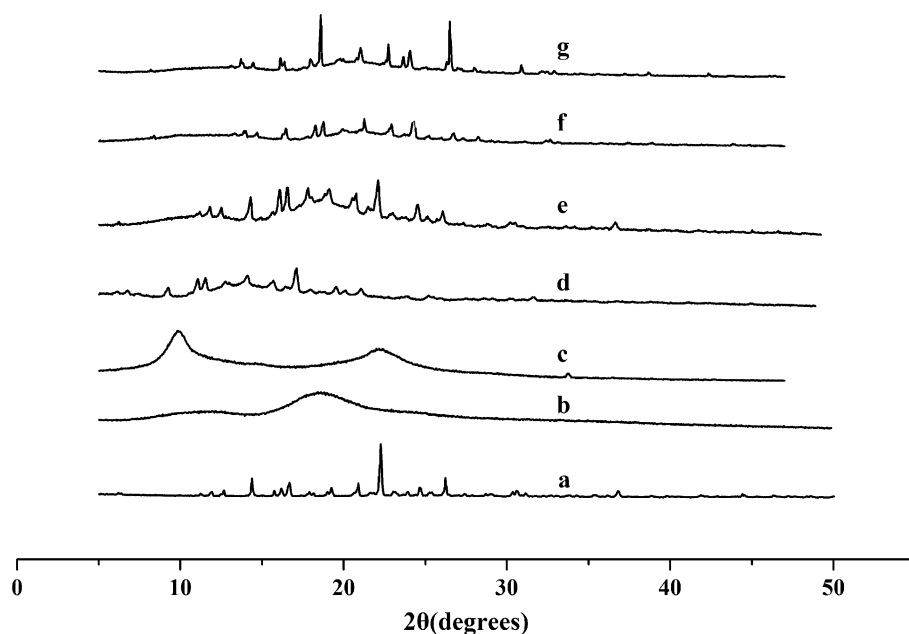

Table 3 ¹H NMR chemical shift data of fenofibrate in inclusion complexes

Fenofibrate	δ (free)	δ (binary complex)	Δδ (ppm)	δ (ternary complex)	Δδ (ppm)
H-1	1.154	1.149	− 0.005	1.130	− 0.024
H-2	1.608	1.602	− 0.006	1.603	− 0.005
H-3	4.982	4.961	− 0.021	4.888	− 0.094
H-4	6.903	6.901	− 0.002	6.899	− 0.002
H-5	7.623	7.624	0.001	7.624	− 0.001
H-6	7.718	7.713	− 0.005	7.708	− 0.010

Table 4 ¹H NMR chemical shift data of HP-β-CD in inclusion complexes

HP-β-CD	δ (free)	δ (binary complex)	Δδ (ppm)	δ (ternary complex)	Δδ (ppm)
H-1	4.831	4.834	0.003	4.977	0.046
H-2	3.220	3.220	0	3.221	0.001
H-3	3.745	3.754	0.009	3.775	0.030
H-4	3.333	3.336	0.003	3.333	0.000
H-5	3.443	3.481	0.038	3.430	− 0.013
H-6	3.612	3.613	0.001	3.615	0.003

the cavity. The chemical shifts of H-3 ($\Delta\delta = 0.009$ ppm in binary complex, $\Delta\delta = 0.030$ ppm in ternary complex) and H-5 ($\Delta\delta = 0.038$ ppm in binary system, $\Delta\delta = -0.013$ ppm in ternary system) protons of HP-β-CD were expected as results of interaction with FNB. This evidence indicates interaction between the FNB and the interior of the

HP-β-CD cavity. The chemical shifts of FNB protons signals were also reported (Table 3), the results show the variations of protons induced by HP-β-CD. Some of the FNB protons signals were overlapped in the spectra of complexes and the signals were much weaker compared with the pure drug. The most obvious change of FNB protons were H1 (CH_3−) and H3 (–CH–O) in the group of isopropyl connected with the ester group. Combined with the displacement of O–H groups in FI-IR spectrum of the complexes, it was confirmed that this attributed to the interaction of water molecules inside the cavity of HP-β-CD with the ester group. The presence of HPMC has aggravated this phenomenon. The results of ¹H NMR were also consistent with the results of DSC and FI-IR analysis which demonstrate formation of FNB complexes.

In vitro dissolution test

The dissolution rate of the drug in the dissolution medium is also an effective parameter to measure the biological activity of the drugs because it is closely related to the bioavailability of the drug. The dissolution rate of the samples was shown in Fig. 6. The cumulative release percentage of FNB in ternary system reached to 90% in 20 min (Fig. 6c) while only 24% in pure drug (Fig. 6a) and 60% in binary system (Fig. 6b). The significant improvement in the dissolution efficiency of the inclusion complexes should be ascribed to complexes formation, and the higher dissolution rate of the ternary system can be attributed to the polymer assisted enhanced complexation in ternary system. This also demonstrates that the HPMC can enhance the complexation of HP-β-CD and FNB.
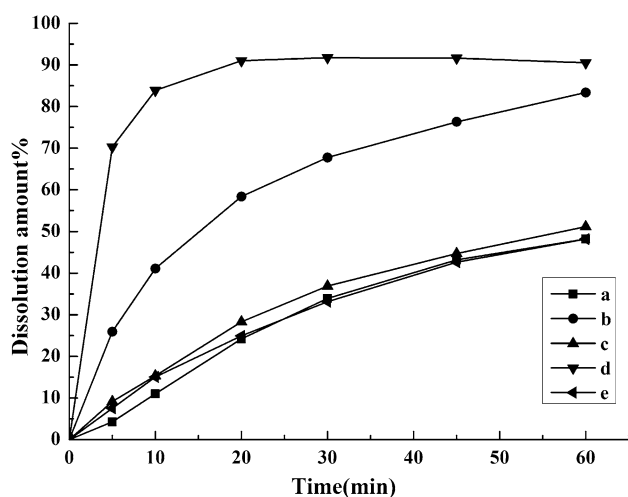
Fig. 6 Release rate of FNB (**a**), binary complex (**b**), ternary complex (**c**), binary physical mixture (**d**), and ternary physical mixture (**e**) in the solution of 0.5% SDS at 37 °C

Conclusion

The phase solubility study shows the formation of inclusion complexes (molar ratio of 1:1), and the complexation efficiency of FNB and HP-β-CD improved significantly in the presence of HPMC. The results of FT-IR, XPRD, DSC and ^{1}H NMR analysis show the formulation of inclusion complexes. In addition, the in vitro dissolution tests suggest that the ternary system is more effective to improve the in vitro dissolution rate of FNB. Therefore, the presence of HPMC has a good effect on the complexation of FNB and HP-β-CD.

Compliance with ethical standards

Conflict of interest The authors declares that they have no conflict of interest.

References

1. Sanganwar, G.P., Gupta, R.B.: Dissolution-rate enhancement of fenofibrate by adsorption onto silica using supercritical carbon dioxide. Int. J. Pharm. **360**, 213–218 (2008)
2. Steiner, G.: Fenofibrate for cardiovascular disease prevention in metabolic syndrome and type 2 diabetes mellitus. Am. J. Cardiol. **102**, 28L (2008)
3. Huang, Q.P., Wang, J.X., Zhang, Z.B., Shen, Z.G., Chen, J.F., Yun, J.: Preparation of ultrafine fenofibrate powder by solidification process from emulsion. Int. J. Pharm. **368**, 160–164 (2009)
4. Zhong, L., Zhu, X., Luo, X., Su, W.: Dissolution properties and physical characterization of telmisartan–chitosan solid dispersions prepared by mechanochemical activation. AAPS PharmSciTech. **14**, 541–550 (2013)
5. Silva, C.V., Barbosa, J.A., Ferraz, M.S., Silva, N.H., Honda, N.K., Rabello, M.M., Hernandes, M.Z., Bezerra, B.P., Cavalcanti, I.M., Ayala, A.P.: Molecular modeling and cytotoxicity of diffractaic acid: HP-β-CD inclusion complex encapsulated in microspheres. Int. J. Biol. Macromol. **92**, 494–503 (2016)
6. Aloisio, C., Antimisiaris, S.G., Longhi, M.R.: Liposomes containing cyclodextrins or meglumine to solubilize and improve the bioavailability of poorly soluble drugs. J. Mol. Liq. **229**, 106–113 (2017)
7. Du, F., Meng, H., Xu, K., Xu, Y., Luo, P., Luo, Y., Lu, W., Huang, J., Liu, S., Yu, J.: Colloids: CPT loaded nanoparticles based on beta-cyclodextrin-grafted poly(ethylene glycol)/poly (L-glutamic acid) diblock copolymer and their inclusion complexes with CPT. Surf. B Biointerfaces **113**, 230–236 (2014)
8. Pereira, R.A., Anconi, C.P., Nascimento Jr, C.S., De Almeida, W.B., Dos Santos, H.F.: Stability and spatial arrangement of the 2,4-dichlorophenoxyacetic acid and β-cyclodextrin inclusion compound: a theoretical study. Chem. Phys. Lett. **633**, 158–162 (2015)
9. Jun, S.W., Kim, M.S., Kim, J.S., Park, H.J., Lee, S., Woo, J.S., Hwang, S.J.: Preparation and characterization of simvastatin/hydroxypropyl-beta-cyclodextrin inclusion complex using supercritical antisolvent (SAS) process. Eur. J. Pharm. Biopharm. **66**, 413 (2007)
10. Fraceto, L.F., Grillo, R., Sobarzo-Sánchez, E.: Cyclodextrin inclusion complexes loaded in particles as drug carrier systems. Curr. Top. Med. Chem. **14**, 518 (2014)
11. Liao, Y., Zhang, X., Li, C., Huang, Y., Lei, M., Yan, M., Zhou, Y., Zhao, C.: Inclusion complexes of HP-β-cyclodextrin with agomelatine: preparation, characterization, mechanism study and in vivo evaluation. Carbohydr. Polym. **147**, 415–425 (2016)
12. Raza, A., Sun, H., Bano, S., Zhao, Y., Xu, X., Tang, J.: Preparation, characterization, and invitro anti-inflammatory evaluation of novel water soluble kamebakaurin/hydroxypropyl-β-cyclodextrin inclusion complex. J. Mol. Struct. **1130**, 319–326 (2017)
13. Ribeiro, L., Loftsson, T., Ferreira, D., Veiga, F.: Investigation and physicochemical characterization of vinpocetine-sulfobutyl ether beta-cyclodextrin binary and ternary complexes. Chem. Pharm. Bull. **51**, 914–922 (2003) (Tokyo)
14. Sauceau, M., Rodier, E., Fages, J.: Preparation of inclusion complex of piroxicam with cyclodextrin by using supercritical carbon dioxide. J. Supercrit. Fluids. **47**, 326–332 (2008)
15. Rao, M., Bajaj, A., Khole, I., Munjapara, G., Trotta, F.: In vitro and in vivo evaluation of β-cyclodextrin-based nanosponges of telmisartan. J. Incl. Phenom. Macrocycl. Chem. **77**(1-4), 135–145
16. Zhang, M., Li, H., Lang, B., O'Donnell, K., Zhang, H., Wang, Z., Dong, Y., Wu, C., Iii, R.O.W.: Formulation and delivery of improved amorphous fenofibrate solid dispersions prepared by thin film freezing. Eur. J. Pharm. Biopharm. **82**, 534 (2012)
17. Brewster, M.E., Loftsson, T.: Cyclodextrins as pharmaceutical solubilizers. Adv. Drug Deliv. Rev. **59**, 645–666 (2007)
18. Danciu, C., Soica, C., Oltean, M., Avram, S., Borcan, F., Csanyi, E., Ambrus, R., Zupko, I., Muntean, D., Dehelean, C.A.: Genistein in 1:1 inclusion complexes with ramified cyclodextrins: theoretical, physicochemical and biological evaluation. Int. J. Mol. Sci. **15**, 1962–1982 (2014)
19. Ol'Khovich, M.V., Sharapova, A.V., Lavrenov, S.N., Blokhina, S.V., Perlovich, G.L.: Inclusion complexes of hydroxypropyl-β-cyclodextrin with novel cytotoxic compounds: Solubility and thermodynamic properties. Fluid Phase Equilib. **384**, 68–72 (2014)
20. Da, Z., Jianqiang, Z., Kunming, J., Ke, L., Yangwei, C., Shaoping, P., Yi, J., Jun, L.: Preparation, characterisation and antitumour activity of β-, γ- and HP-β-cyclodextrin inclusion complexes of oxaliplatin. Spectrochim. Acta Part A. **152**, 501–508 (2016)

21. Patel, A.R., Vavia, P.R.: Preparation and evaluation of taste masked famotidine formulation using drug/β-cyclodextrin/polymer ternary complexation approach. AAPS PharmSciTech. **9**, 544–550 (2008)

22. Liu, B., Zhao, J., Liu, Y., Zhu, X., Zeng, J.: Physicochemical [corrected] properties of the inclusion complex of puerarin and glucosyl-β-cyclodextrin. J. Agric. Food Chem. **60**, 12501 (2012)

23. Zhang, W., Gong, X., Cai, Y., Zhang, C., Yu, X., Fan, J., Diao, G.: Investigation of water-soluble inclusion complex of hypericin with β-cyclodextrin polymer. Carbohydr. Polym. **95**, 366–370 (2013)

24. Chowdhry, B.Z., Leharne, S.A., Badwan, A.A.: Novel inclusion complex of ibuprofen tromethamine with cyclodextrins: physicochemical characterization. J. Pharm. Biomed. Anal. **50**, 449–458 (2009)

25. Roy, A., Saha, S., Roy, M.N.: Exploration of inclusion complexes of probenecid with α and β-cyclodextrins: Enhancing the utility of the drug. J. Mol. Struct. **1144**, 103–111 (2017)

26. Sailaja, U., Thayyil, M.S., Kumar, N.S.K., Govindaraj, G.: Molecular dynamics of amorphous pharmaceutical fenofibrate studied by broadband dielectric spectroscopy. J. Pharm. Anal. **6**, 165–170 (2016)

27. Linares, M.S., Longhi, M.R.: Effects of hydroxypropyl-beta-cyclodextrin on the chemical stability of a naphthoquinone in aqueous solutions. Pharmazie. **58**, 32 (2003)